Simulation of the Inclined Impinging Cooling in a Channel with Cross Flow

Khudheyer S. Mushatet
College of Engineerin- Thi-Qar University

Abstract:

In this work, a numerical investigation has been conducted to analyze the turbulent flow and heat transfer of the inclined impinging jets in a channel with cross flow. The impinging jets were inclined towards the upstream side and the angle of inclination was changed from 30° to 90°. For this flow configuration, two cases were considered for the channel, one free ribs and the other with rib turbulators. The characteristics of air flow and heat transfer are analyzed under different parameters such as the angles of inclination, size of jets, number of jets, pitch between jets and jet and channel Reynolds numbers. A finite volume method is used to integrate the continuity, fully elliptic Reynolds average Navier-Stockes and energy equations. In turns, these equations are used to simulate the flow and thermal fields in the considered computational model. The effects of turbulence are treated using the standard k-ε model. The wall effects are modeled using the wall function laws. The computed results indicate that the recirculation regions are increased with the increase of inclination angle (α). Also the results show that the variation of the local Nusselt number, turbulent kinetic energy are significantly effected with the increase of size and number of jets, the distance between jets and jet and channel Reynolds numbers. The validation of the present numerical scheme is accomplished through a comparison with available published results.

المستخلص:

في هذا العمل تم انجاز دراسة عددية لتحليل خصائص الجريان الضطرابي وانتقال الحرارة للمنافث التصادمية في مجرى هوائي بوجود جريان متقاطع. تميل المنافث التصادمية باتجاه مجرى الجريان الرئيسي وقد درست ثلاث قيم من زوايا الميلان $\left(30^\circ \le \alpha \le 90^\circ\right)$. تضمنت الدراسة الحالية اختبار حالتين، واحدة لمجرى هوائي بدون عوارض والثانية لمجرى هوائي مع وجود عوارض. تم تحليل خصائص الجريان تحت تأثير عوامل مختلفة مثل زوايا الميلان، عدد وحجم المنافث التصادمية والمسافة بين هذه المنافث وعدد رينولدز للمجرى االرئيسي والمنفث التصادمي. أستخدم اسلوب الحجم المحدد لتكامل معادلات الأستمرارية و نافير-ستوكس والطاقة وهذه المعادلات تستحدم بدورها لنمذجة مجال الجريان وانتقال الحرارة للمجال الحسابي المدروس. عولجت تأثيرات الأضطراب باستخدام نموذج k-є بينما تأثيرات الجدار عولجت باستخدام قانون دالة الجدار. أوضحت النتائج المستحصلة ان حجم مناطق اعادة التدويرقد زاد مع زيادة زوايا الميلان. أيضا بينت النتائج أن معدل انتقال الحرارة والطاقة الحركية للأضطراب قد تاثر بصورة ملحوظة مع تغير حجم وعدد المنافث التصادمية والمسافة بين المنافث وكذلك تغير عدد رينولدز للمنافث التصادمية وللمجرى الرئيسي. تم التأكد من صحة الطريقة الحالية من خلال المقارنة مع النتائج المنشورة.

1. Introduction

Impingement cooling are used in a wide range of industrial and engineering applications such as turbine blade cooling, cooling of electronic components,

tempering of glass and drying papers. Impinging jets have received considerable attention in many research investigations because they can remove a large amounts of heat over a small area consequently producing high local heat transfer. In some applications of impinging cooling, slot jets have advantages over circular jets since a slot jet has a large impingement region. The increase of the distance between the jet and the surface leads to decrease the local heat transfer significantly, so the remedy is adopting multiple impinging jets or using a rib roughened walls. Thus it is important to show the effect of the rib turbulators on the impinging flow field and heat transfer. For slot impinging jets, extensive experimental and numerical studies has been found. Law and Masliyah [1], Chou and Hung [2] and Lee et al. [3] performed numerical investigation on low Reynolds number impinging jets. The cause behind using low Reynolds number was to avoid a hydrodynamic pressure caused by the impinging on the surface. Behna et al [4], Cooper et al. [5], Park and Sung [6] presented a numerical studies on high Reynolds number impinging jets with different turbulenc models. To improve heat transfer distribution in the impingement region, impinging jets were studied with different angles of attacks. Beitelmal et al. [7], Yang and shyu [8] and EL-Gabry et al. [9] used CFD models to predict the heat transfer distribution on a smooth surface under an array of angled impinging jets with cross flow. Different angles of attack and conjugate conduction in the boundary were included. The k-ϵ model and yang-Shih model were examined. The study showed that yang-Shih model superior to k-ϵ model. Craft et al. [10] applied four turbulence models to the numerical prediction of the turbulent impinging jets discharged from a circular pipe. Shou et al. [11] studied the effect of jets in cross flow on impingement heat transfer from rib-roughened rotating curved square duct. The curvature of the duct, rib height, pitch to height ratio (p/e) was fixed while the jet Reynolds and stream cross flow were changed. Concerning the flow and heat transfer characteristics inside a channel roughened with rib turbulators, Web et al.[12], Lio and chen [13] and Rau et al. [14] and Hane and Park [15] studied the turbulent flow and heat transfer in a channel with rib turbulators. The main objective of these studies was to obtain the heat transfer characteristics and friction factor. Saidi and Sunden [16] investigated the turbulent flow and heat transfer in three dimensional rib-roughened channels using simple eddy viscosity model and algebraic stress model. Their study showed that the algebraic stress model has superiority over the eddy viscosity model for the prediction of the flow field but the mean thermal predictions are not very different. Also Viswanathan and Tafti [17-18], Murtadha and Mochizulki [19] and Watanabi and Takahashi [20] studied the turbulent flow in the channels roughened with ribs. In this work a numerical investigation to predict the turbulent flow and heat transfer characteristics of multiple angled impinging slot jets in a cross channel flow has been reported. As shown in Fig.1, the jet has a width (B), inclination angle (α) towards the upstream side, the rib has a thickness (W), the height of the channel is (H). The channel height to a jet width ratio (H/B) and the jet width to the rib thickness ratio(B/W) are changed for different values. Different jet Reynolds numbers and a channel cross flow Reynolds numbers are examined. The jet Reynolds number is based on the jet width (B) and the channel Reynolds number on the channel height(H). The effect of the inclination angle of the impinging jets on flow and heat transfer is investigated. To the knowledge of the author, till now there is no published study on inclined multiple impinging cooling in a

channel with cross flow. The objective of this study is to show the effect of impinging jets inclination angle on the flow and heat transfer characteristics along the mentioned two configurations of the channel.

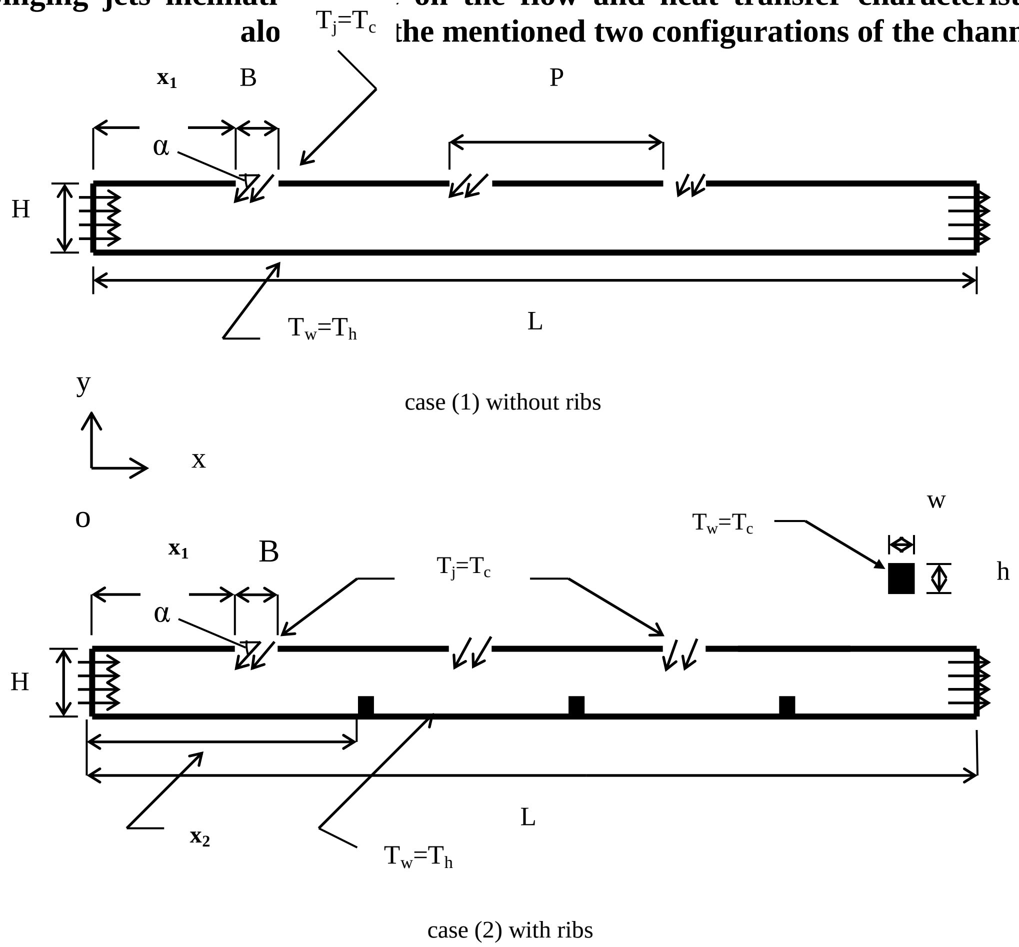

Fig.1. problem description with H=0.05 m, L=0.4 m, H/B=11, h/H=0.38, W/h=2, P/B=4, x_1=0.0492m, x_2=0.0826m, e=0.11m

2. Mathematical model

The turbulent flow of air and heat transfer are described mathematically by the time-averaged Navier-Stockes equations. To simplify the numerical simulation by using a two dimensional mathematical model along with a finite volume scheme, the thermo physical properties of air are assumed constant and Boussinesq approximation is valid. Thus the Reynolds average Navier-Stokes and energy equations in tensor form can be written as:

$$\frac{\partial}{\partial x_i}\left(\rho U_i\right)=0 \qquad \textbf{(1)}$$

$$\frac{\partial U_i U_j}{\partial x_j} = \frac{-\partial P}{\partial x_i} + \frac{\partial}{\partial x_j}\left(\mu \frac{\partial U_i}{\partial x_j} - \overline{\rho u_i u_j}\right) \qquad \textbf{(2)}$$

$$\frac{\partial U_i T_j}{\partial x_j} = \frac{\partial}{\partial x_j}\left(\frac{\mu}{\Pr}\frac{\partial T_i}{\partial x_j} - \overline{\rho u_i t_j}\right) \qquad \textbf{(3)}$$

The turbulent stresses $\overline{\rho u_i u_j}$ and turbulent heat fluxes $\overline{\rho u_i t_j}$ should be modeled in order to close the considered governing equations. One of the most widely turbulence models is the standard k-ϵ model. This model has the ability to handle complex high Reynolds number flows in much less time than other complicated models. This model solves two transport equations one for the turbulent kinetic energy and the other for the dissipation rate of the turbulent kinetic energy, Launder and Spalding [22], as shown bellow:

$$\frac{\partial \rho k U_i}{\partial x_j} = \frac{\partial}{\partial x_j}\left[\left(\mu + \frac{\mu_t}{\sigma_k}\right)\frac{\partial k}{\partial x_j}\right] + \rho(G_b - \varepsilon) \qquad \textbf{(4)}$$

$$\frac{\partial \rho \varepsilon U_j}{\partial x_j} = \frac{\partial}{\partial x_j}\left[\left(\mu + \frac{\mu_t}{\sigma_\varepsilon}\right)\frac{\partial \varepsilon}{\partial x_j}\right] + \rho\frac{\varepsilon}{k}\left(C_{1\varepsilon} G_b - C_{2\varepsilon}\varepsilon\right) \qquad \textbf{(5)}$$

where the shear production term, (G_b) are define as:

$$G_b = \mu_t\left(\frac{\partial u_i}{\partial x_j} + \frac{\partial u_j}{\partial x_i}\right)\frac{\partial u_i}{\partial x_j} \qquad \textbf{(6)}$$

and the turbulent viscosity is define as:

$$\mu_t = \rho c_\mu \frac{k^2}{\varepsilon} \qquad \textbf{(7)}$$

the model coefficients are (σ_k ; σ_ϵ ; $C_{1\epsilon}$; $C_{2\epsilon}$; $C\mu$) = (1.0 , 1.3 , 1.44 , 1.92 , 0.09) respectively. The flow parameters at inlet are described as follows:

$k_{in} = 1.5 I_u^2 U_{in}^2$, $k_j = 1.5 I_u^2 U_j^2$, $I_u = 2\%$

$\varepsilon_{in} = k_{in}^{1.5} / \lambda H$, $\varepsilon_j = k_j^{1.5} / \lambda B$, $\lambda = 0.005$

$\mathrm{Re}_{in} = \frac{U_{in} H}{\nu}$, $\mathrm{Re}_j = \frac{U_j B}{\nu}$, $T_{in} = T_c$ **=25Ċ,** $T_j = T_c$ **=25 Ċ,**

where k_{in}, k_j, U_{in}, U_j, T_{in}, T_j are the turbulent kinetic energy, velocity and temperature at a channel inlet and a slot jet respectively.

At the walls, no slip conditions are imposed; U=V=0., k = 0., $\frac{\partial \varepsilon}{\partial y} = 0.$, $T_w = T_h$=50 Ċ. While T_c=25 Ċ is assigned to the rib turbulators. The local Nu along the bottom hot wall is expressed as $Nu = \frac{\partial \theta}{\partial Y}$, at y=0., $\theta = \frac{T - T_c}{T_h - T_c}$, $Y = \frac{y}{H}$

To obtain a smooth transition at the channel exit, the second derivative of the considered dependent variables is equal to zero (i.e. $\frac{\partial^2 U}{\partial x^2} = 0$**,……etc). To remedy the large steep gradients near the walls of the channel and the rib turbulators, there are two approaches. In the first approach, the turbulence model is modified to enable this region to be resolved with a fine mesh. In the second approach, the wall function laws used by Versteege [23] are used to handle the mean velocities, temperature along with the turbulence quantities. This approach is adopted here because it is economical, popular, reasonable accurate and saves computational resources.**

3. Numerical procedure

In this study, the numerical computations are performed on non-uniform staggered grid system. A finite volume method (FVM) described by the following formula is adopted to integrate the considered governing equations (1) to (5).

$$\int_{cv} (\rho\phi u) dv = \int_{cv} div(\Gamma grad\phi) dv + \int_{cv} S_\phi dv \qquad \textbf{(8)}$$

This gives a system of discretization equations which means that the system of elliptic partial differential equations is transformed in to a system of algebraic equations. Then the solution of these transformed equations is performed by implicit line by line Guass elimination scheme. An elliptic finite volume computer code is developed to attain the results of the numerical procedure through using pressure-velocity coupling (SIMPLE algorithm) [23]. This code is based on hybrid scheme. Due to this strong coupling and non-linearity inherent in these equations, relaxation factors are needed to ensure convergence. The relaxation factors used for velocity components, pressure , temperature and turbulence quantities are 0.5, 1, 0.7, 0.7 respectively. However these relaxation factors have been adjusted for each case studied to accelerate the convergence criterion defined as the relative deference of every dependent variable between iteration steps. A typical run of 5000 takes about 215 CPU seconds on PENTIUM 4 computer is done. To ensure that the turbulent fluid flow solutions are not significantly affected by the mesh, the numerical simulations are examined under different grid sizes ranging from (62×28) until (82×52) control volumes. Any additional increase in grid points on (62×28) does not significantly effect on the result

4. Results and discussion

The computed results for 2D turbulent flow and heat transfer of the inclined impinging cooling in a channel with cross flow are presented as follows:

Figs 2-4 show the effect of jet inclination angle on the distribution of computed velocity vectors for multiple impinging slot jets in cross flow. It is evident that the recirculation regions formed between the jets are increased with the increase of number of impinging slot jets. Also this increase includes the re-attachment length. It is clear that the angle 90° **gives the larger recirculation regions. As the Figures show, apart of the flow of impinging jets form re-circulating zones between the jets and other part push the cross flow towards the wall. Consequently, the main flow is accelerated and the channel flow passage**

becomes narrower. This situation will enhance the heat transfer as shown in the next sections. It is important to mention that the small value of angle of inclination, plays passive role because it pushes only the flow near the upper wall. Figs.5-6 demonstrate the effect of angle of inclination on the flow field for increasing the slot jet width (H/B). It is clear that the recirculation regions behind each jet are increased with the increase a slot jet width and one can see that the angle of inclination have a significant effect on the size and reattachment lengths of the impinging jets. As the Figures show, when $\alpha = 30^\circ$, the effect of impinging jets are limited to the regions near the upper wall and consequently decreasing the recirculation regions behind each jet. However these recirculation regions are increased with the increase of a slot jet width (H/B). This flow structure is dominant for all the studied cases. The flow of impinging jets are strongly affected the main cross stream when H/B=2.5 for all the studied cases. However this situation is tested here for the considered angles of inclination and number of jets. In general, the velocity of main channel flow near the hot wall is increased with decreasing the ratio H/B (increasing the width of impinging jet) since the channel flow passage becomes narrower. This shrinking will increase the velocity gradient in the vicinity of the wall consequently increasing the shear stresses. When the velocity gradients are increased, the turbulence effects are increased and this has a direct effect on the enhancement of heat transfer as shown in the next sections. The effect of a slot jet width (H/B) on the variation of local Nusselt number is depicted in Figures 7-8 for different angles of inclination. As shown in Fig.7.a, the local Nusselt number is increased with the increase of number of jets and with the increase of jet width. Also the Nu is increased with the increase of jet width as in (a) and (b) for $\alpha = 30^\circ$. The reason behind this is that the recirculation regions are increased behind each jet and that leads to increase the impinging flow towards the hot wall along with increasing the turbulence effects consequently increasing the heat transfer enhancement. However the enhancement will enhance with the increase of angle of inclination. As shown in Fig.8(a and b). This behavior is dominant for all the studied angles of inclination. The effect of changing the ratio of pitch to jet width (P/B) on the computed flow field for different angles of inclination is exhibited in Fig.9. As velocity vectors, it can be seen that the recirculation regions are decreased with increasing the ratio (P/B) and the inclination angle (α) has a noticeable effect in which this recirculation regions are become smaller and the re-attachment length is shorter as shown in (a and b). However the cooling of the wall in the first jet at P/B=4 is stronger. This trajectories of the impinging jets forced the cross flow towards the wall under impinging areas and between the jets are clearly seen in c and d as stream lines. The stream lines are seem to be deflected more toward the wall in case (c) rather than (d). However this increase become less down stream the second jet. This behavior is enhanced with the increase of the angle of inclination (α) as shown in e and f as velocity vectors and g and h as stream lines in which the recirculation regions and reattachment length besides the cooling of the hot wall is larger. The cause behind this , is that when $\alpha = 90^\circ$, the impinging flow is directly impinging normal to the main stream while at $\alpha = 30^\circ$, the impinging flow is divided in to two parts, one is vertical and the other is inclined opposite the main stream and that waken the effect of impinging cooling. This behavior explain the variation of Nusselt number with cross flow for cases K&L, where in

case (c), for $\alpha = 30^\circ$, the Nusselt number for P/H=4 increases at a limited region while when P/H=12, We can see increase in Nusselt number. This behavior is different for $\alpha = 90^\circ$ where the Nusselt number at P/B=4 increases for considerable distance after that decreases and the Nusselt number at P/B=12 increases. The effect of the presence of rib turbulators on the impinging cooling in cross flow for different angles of inclination is shown in Fig.10as streamlines contours. As the figure shows, one might see that the recirculation regions and the re-attachment length behind each jet are decreased while new recirculation regions and separation of boundary layer are shown due to the existence of ribs. It can be seen here that the recirculation regions between the impinging slot jets are significantly decreased. This is because of the presence of ribs. The impinging jets flow and the cross flow can not deflect directly towards the hot wall where the ribs shift the combined flow and accelerate it downstream the rib forming a recirculation zone. This will enhance the heat transfer too. Thus the presence of ribs has merits and disadvantages. As the figure shows, the increase of the number of ribs increases the turbulence along with the increase of multiple impinging jets as shown in (a,b,c). This is expected to enhance the heat transfer because the turbulence is higher in this combined complex flow. The presence of ribs prevents the deflection of high inertia flow(cross flow plus jets flow) towards the hot wall but the deflection of streamlines occurs at regions between the ribs. The flow is faster above and downstream each rib. As the figure shows, the recirculation regions behind each jet and ribs besides the deflection of streamlines are increased with the increase of inclination angle and $\alpha = 90^\circ$ indicted the best performance. Figs 11-12 presente the velocity vectors and stream lines contours of multiple angled impinging jets in a rib roughened channel for different angles of inclination. The ratio of the channel height to the jet width is decreased to 2.5 and the ratio of the jet width to the rib thickness is decreased to 2. As the figure shows, these ratios have a strong effect on the recirculation regions and reattachment length with regard to the impinging cooling and turbulent cooling. The recirculation regions behind the ribs and jets are noticeably increased. However this increase is larger at the turbulent cooling rather than the impinging cooling. For this combined complex flow, the main flow penetration to the hot wall seems to be stronger and the heat transfer is enhanced as shown in Fig. 13. This cause as a result to increase the mass flow rate of the flow of impinging jets. However the increase of the recirculation regions size between the impinging slot does not reach the recirculation regions in size in the case of the channel without ribs. As a result we expect a heat transfer enhancement is better as shown in Fig.13. This behaviour is seem to be stronger at $\alpha = 90^\circ$ compared with $\alpha = 30^\circ$. As a result we expect a heat transfer characteristics is bettr as shown in Fig.13 where the variation of Nusselt number is depicted. It can be seen that the presence of ribs will increase the Nu because the ribs increase the turbulence and promote the heat exchange with the hot wall and consequently enhance the heat transfer. It can be seen that the local Nusselt number is increased with the increase of angle of inclination (α) for the two jets and decrease with the increase of (α) for three and four jets. The distribution of turbulent kinetic energy for angled impinging jet cooling in a channel roughened ribs for different angles of inclination is found in Fig..14. it is clear that the turbulent kinetic energy is increased at $\alpha = 30^\circ$ and decreased at

$\alpha = 60^\circ$ **after that it increased at** $\alpha = 90^\circ$. **The velocity gradient is less at the channel exit so the kinetic energy is rapidly decreased. The validation of the present code is performed by comparing the present results with available published experimental data as shown in Fig.15. The comparison indicated acceptable agreement. The recirculation zone behind each jet and reattachment length are significantly increased with the increase of the impinging slot jet velocity and cross stream velocity (i.e. Re_j and Re_{in}) as shown in Fig.16. The increase in Reynolds number increase the inertia force and the penetration of the impinging jet flow to the cross flow and consequently enhance heat transfer as shown in Fig.17. This fact is dominant for all angles of inclination. Thus this parameter enhanced the rate of heat transfer as shown in Fig.17. Fig.18. demonstrates the effect of increasing the grid nodes on the distribution of the flow field and Nussult number for three impinging cooling jets. It can be seen that the flow field and Nusselt number do not greatly effected when the mesh exceeding (62×28 node) along with adopting the wall function approximations.**

5. Conclusion

The standard k-ε model along with the finite volume techniques is performed successfully to simulate the turbulent and heat transfer characteristics of the inclined impinging cooling and turbulent cooling inside a channel. Three different values of inclined angles are tested . The large recirculation regions induced by both impinging slot jets and rib turbulators result in high heat transfer enhancement. The size of recirculation regions and reattachment lengths are increased with the increase of angle of inclination. The local Nusselt number is increased with the increase of angle of inclination consequently enhance the rate of heat transfer. The local Nusselt number and size of recirculation zones are increased with the decrease of (B/W) for the studied angles of inclination. The study indicated that the angle of inclination and number of impinging slot jets has a significant effect on the studied parameters.

Nomenclature

B = slot jet width [m]
e = distance between ribs [m]
h = rib height [m]
H = channel height [m]
i, j = tensor notation
I_u = turbulence intensity
k = turbulent kinetic energy [m^2/s^2]
Nu = local Nusselt number
P = jet pitch [m]
p = pressure [N/m^2]
Pr = Prandtl number
Re = Reynolds number
T = temperature [Ċ]
= cold temperature [Ċ] T_c
= hot temperature [Ċ] T_h
= hot wall temperature [Ċ] T_w

= Reynolds stresses [kg/ms^2] $\overline{\rho u_i u_j}$

= turbulent heat fluxes [kg Ċ/m^{2}s] $\overline{\rho u_i t_j}$

U_{in} **= velocity at a channel inlet [m/s]**

U_j **= velocity at a slot jet inlet [m/s]**

W = rib thickness [m]

x, y = cartesian coordinates [m]

Y = dimensionless y-axis coordinate

Greek symbols:

μ = molecular viscosity [kg/ms]

= turbulent viscosity [kg/ms] μ_t

ρ = air density [kg/m^3]

σ_k = turbulent Prandtl number for turbulence

σ_ϵ = turbulent Prandtl number for dissipation of turbulence

Γ = diffusion coefficient [kg/ms]

= dimensionless temperature θ

ϵ = dissipation of turbulent kinetic energy [m^2/s^3]

= source term S_ϕ

References

[1]Law, H.S., Masliyah, J.H., Mass Transfer Due to Confined Laminar Impinging Two Dimensional Jet, Int. J. Heat Mass Transfer, 27: 529-539 (1984)

[2] Chou, Y.J., Hung, Y.H., Impinging Cooling of an Isothermally Heated Surface, ASME J. Heat Transfer 116: 479-482 (1994).

[3] Lee, X.C., Xheng, Q., Zhung, Y., Tia, Y.Q., Numerical Study of Recovery Effect And Impingement Heat Transfer With Submerged Circular Jets of Large Prandtl Number Liquid, Int. J. Heat And Mass Transfer 40: 2647-2653 (1997).

[4] Behnia, M., Parneix, S., Shabany, Y., Durby, P.A., Numerical Study of Turbulent Heat Transfer in Confined And Unconfined Impinging Jets, Int. J. Heat Fluid Flow, 20: 1-9 (1999).

[5] Cooper, D., Jackson, C., Launder, B.E., Liao, G.X., Impingement Jet Studies For Turbulence Model Assessment-I Flow Field Experiments, Int. J. Heat and Mass Transfer, 36: 2675-2684 (1993)

[6] Park, T.S., Sung, H.j., Development of Near Wall Turbulence Model and Application to Jet Impingement Heat Transfer, Int. J. of Heat Fluid Flow, 22: 10-18 (2001).

[7] Beitmal, A.H., Saad, M.A., Patel, C.D., Effects of Surface Roughness on The Average Heat Transfer of An Impinging Air Jet, International Communications in Heat and Mass Transfer, 27: 1-12 (2000).

[8] Yang, Y.T., Shyu, C.H., Numerical Study of Multiple Impinging Slot Jets With An Inclined Confinement Surface, Numerical Heat Transfer, Part A, 33: 23-37 (1999).

[9] EL-Gabry, Lamyaa, A., Kamiski, Deborah, A., Numerical Investigation of Jet Impingement With Cross Flow-Comparison of Yang-Shih And standard k-є Turbulence Models, Numerical Heat Transfer, Part A, 47: 441-469 (2005).
[10] Craft, T.G., Graham, L.G.W., Launder, B.E., Impinging Jet Studies For Turbulence Model Assessment-II- An Examination of The performance of Four Turbulence Models, Int. J. Heat and Mass Transfer, 36: 2685-2697 (1993).
[11] Shou Shing Hsieh, Jung-Tai Huang, Huang-Hsiu Tsai, Impingement Cooling in A Rotating Square Annular Duct With Cross Flow Effect From Rib-Roughened Surface, J. Heat and Mass Transfer, 39, (2003).
[12] Web, R.L., Eckert, E.R.G., Goldsten, R.J., Heat Transfer and Friction in Tubes With Repeated Rib Roughness, International Journal of Heat and Mass, 14: 601-617, (1984).
[13] Lio, T.M., Hwang, G.G. , Chen, S.H., Simulation and Measurements of Enhanced Turbulent Heat Transfer in Channels With Periodic Ribs on One Principal Wall, International Journal of Heat Mass Transfer, 36: 507-507, (1993).
[14] Rau, G., Cakan, M., Moeller, D., Arts, T., The Effect of Periodic Ribs on The Local Aerodynamics and Heat Transfer Performance of A Straight Cooling Channel, ASME Journal of Turbomachinery,120; 368-375, (1988).
[15] Han, J.C, Heat Transfer and Friction Characteristics in Rectangular Channels With Rib Turbulators, ASME Journal of Heat Transfer,110: 91-98, (1988).
[16] Saidi, A., Sunden, B., Numerical Prediction of Turbulent Convection Heat Transfer in Square Ribbed Ducts, Numerical Heat Transfer, Part A, 38: 67-88, (2000).
[17] Viswanathan, A.k., Tafti, D.K., Detached Eddy Simulation of Turbulent flow and Heat transfer in Ribbed Duct, ASME Journal of Fluid Engineering, 127: 888-896, (2005).
[18] Viswanathan, A.k., Tafti, D.K., Detached Eddy Simulation of Turbulent Flow and Heat transfer in Two-Pass Internal Cooling Duct, International Journal of Heat and Fluid Flow, 27: 1-20, (2006).
[19] Murtadha, A. and Mochizuki, S.,Large Eddy Simulation With A Dynamics Sub Grid-Scale Model of Turbulent Flow in Orthogonally Rotating Rectangular Duct With Transverse Rib Turbulators, International Journal of Heat Transfer, vol. 43, 1243-1259, (2001).
[20] Watanabe, K. and Takahashi, T. , Large eddy simulation of fully developed ribbed channel flow and heat transfer, Proc. ASME Turbo Expo, 2002-GT-30203.
[21] Ichimiya, K., Hosaka, N., Experimental Study of Heat Transfer Characteristics Due To Confined Impinging Two Dimensional Jet, Exp. Thermal and Fluid Science, 5: 803-807, (1992).
[22] Launder, B.E., Spalding, D.B., Lectures in Mathematical Model of Turbulence, Academic Press, London and NewYork, (1972).
[23] Versteege, H.K., Malalasekera, W., An Introduction of Computational Fluid Dynamics, Hemisophere Publishing Corporation, United State of America, 1995.

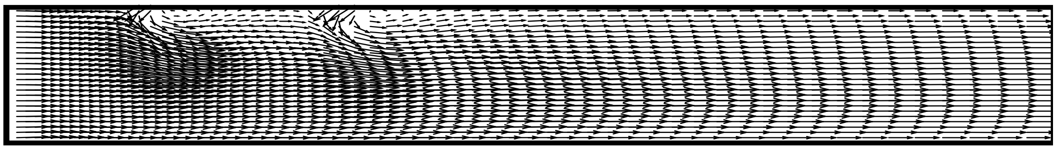

a. $\alpha = 30^\circ$

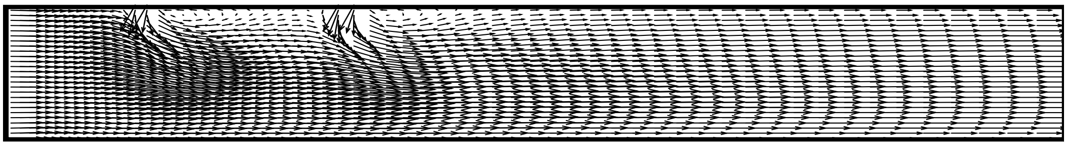

b. $\alpha = 60^\circ$

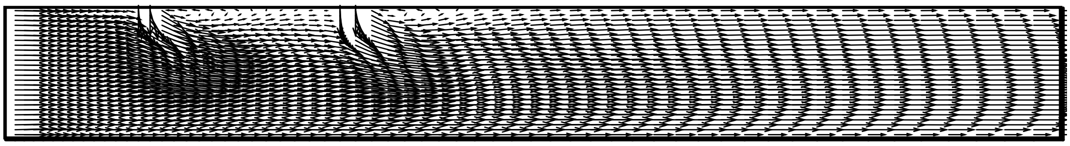

c. $\alpha = 90^\circ$

Fig.2 computed velocity vectors of 2 jets for different jet inclination angles, Re_j =13517, Re_{in}= 16896, H/B=11, P/B=4.

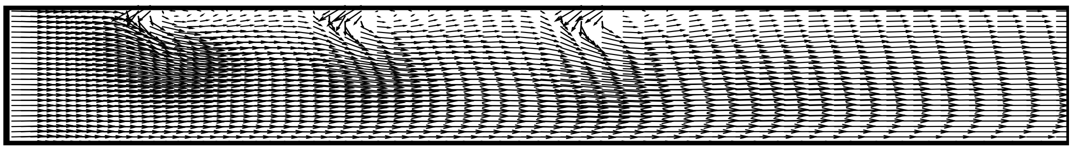

(a) $\alpha = 30^\circ$

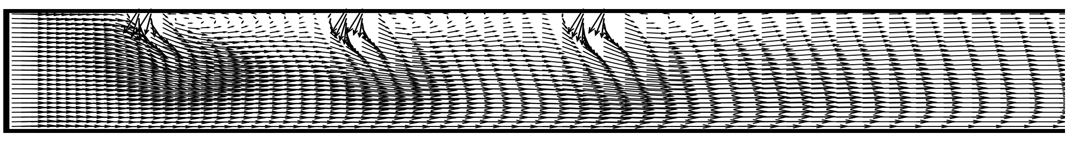

(b) $\alpha = 60^\circ$

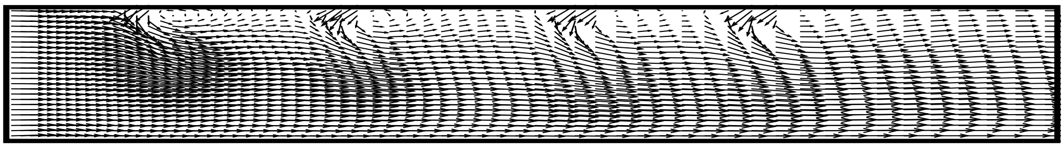

a. $\alpha = 30^\circ$

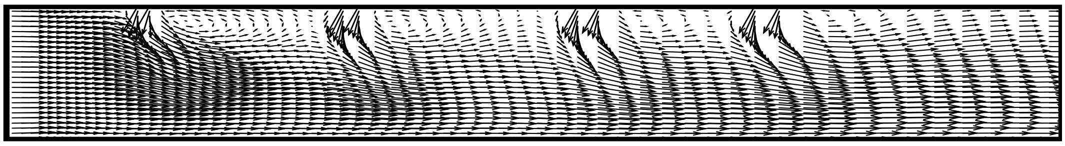

b. $\alpha = 60^\circ$

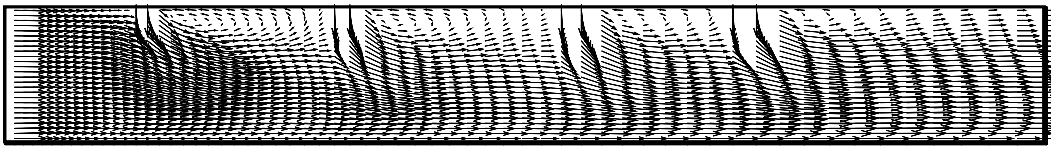

c. $\alpha = 90^\circ$

Fig.4 computed velocity vectors of 4 jets for different jet inclination angles, Re_j =13517, Re_{in}= 16896, H/B=11, P/B=4.

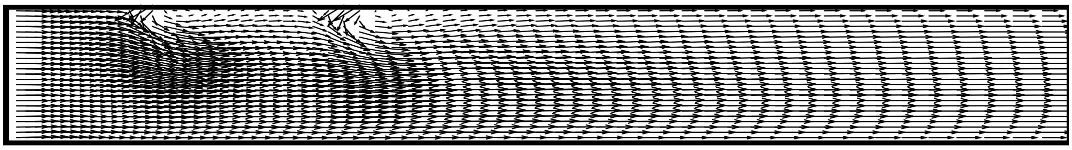

a. 2 jets, H/B=11

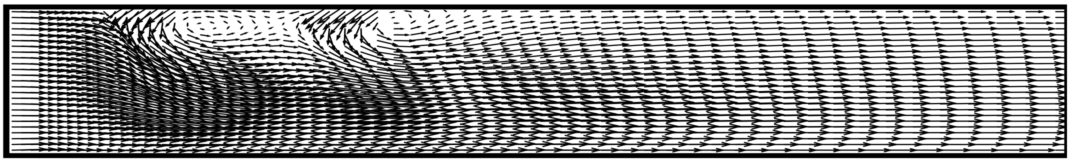

b. 2 jets, H/B=2.5

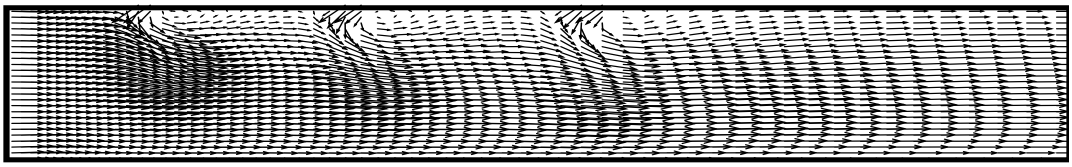

c. 3 jets, H/B=11

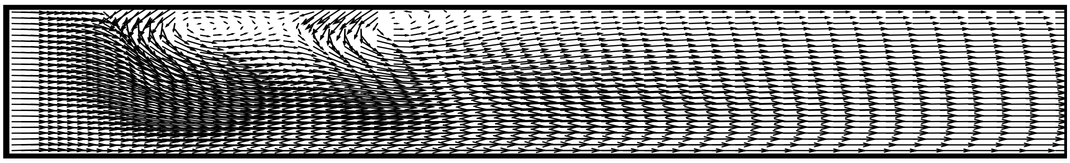

Fig.5. effect of a slot jet width on the flow field for 2 slot jets, Re_j =13517, $\alpha = 30^\circ$

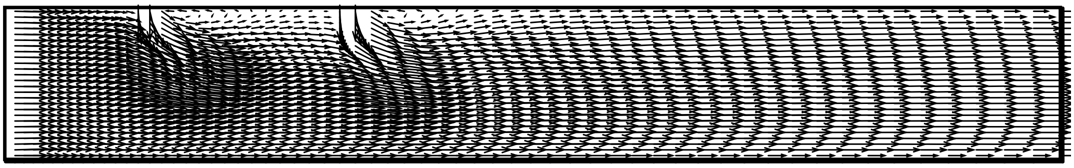

a. 2 jets, H/B=11

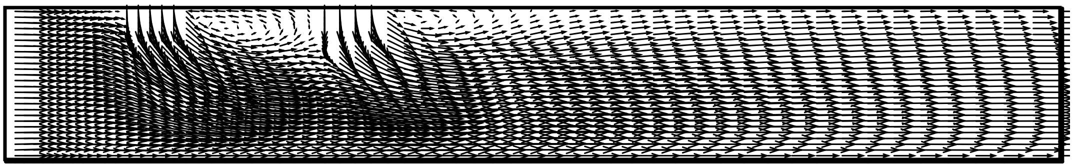

b. 2 jets, H/B=2.5

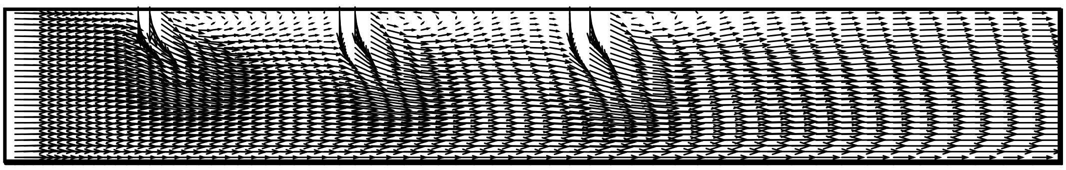

c. 3 jets, H/B=11

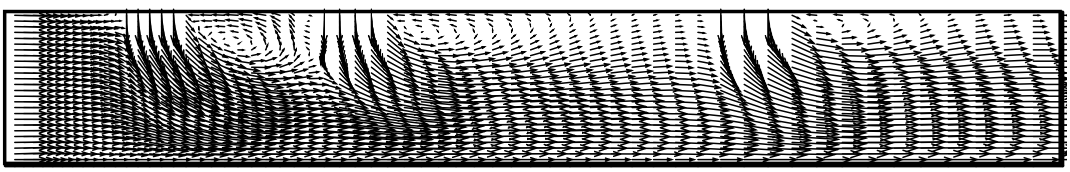

d. 3 jets, H/B=2.5

Fig.6. effect of a slot jet width on the flow field for 2 slot jets, Re_j =13517, $\alpha = 90^\circ$

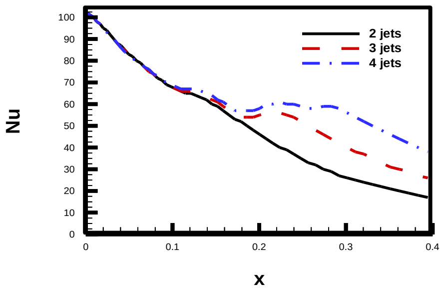

a. Multiple jets, H/B=11

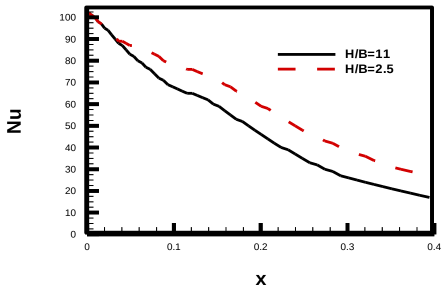

b. 2 jets

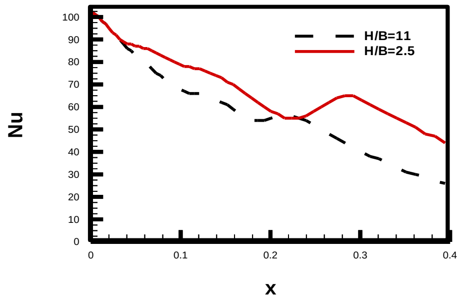

c. 3 jets

Fig.7 effect of a slot jet width on Nu variation, Re_j=13517, Re_{in}=16896, P/B=4, $\alpha = 30^{\circ}$

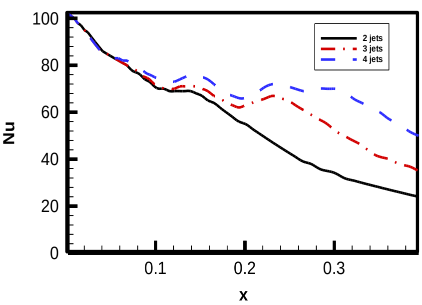

a. multiple jets with H/B=11

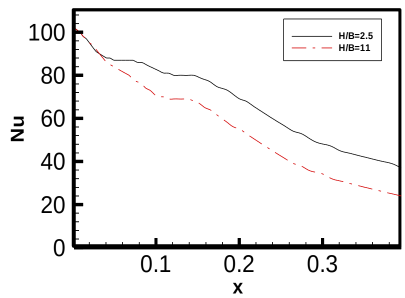

b. 2 jets

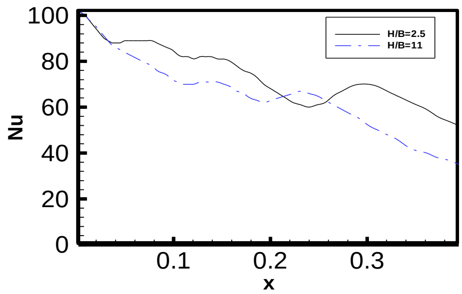

c. 3 jets

Fig.8 effect of a slot jet width on Nusselt number variation, Re_i =13517, Re_{in}= 16896, P/B=4, $\alpha = 90^{\circ}$

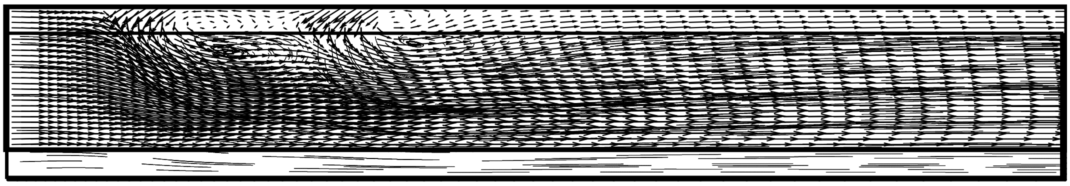

$\alpha = 30^{\circ}$

g. streamlines, P/B=4, $\alpha = 90^{\circ}$

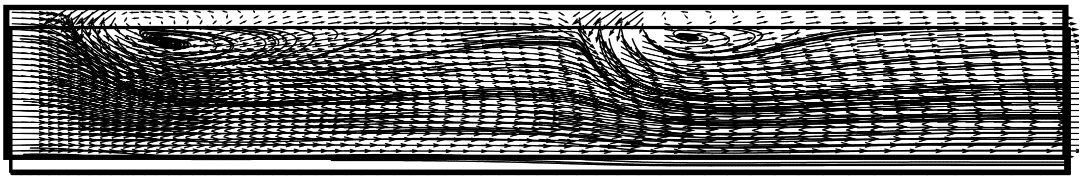

h. streamlines, P/B=12, $\alpha = 90^{\circ}$ 30°

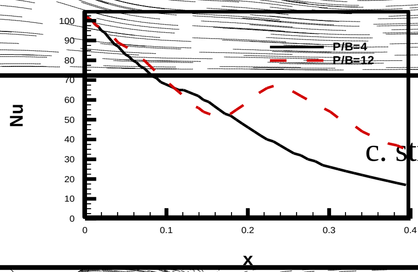

c. streamlines, P/B=4, $\alpha = 30^{\circ}$

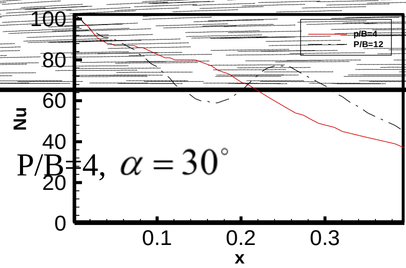

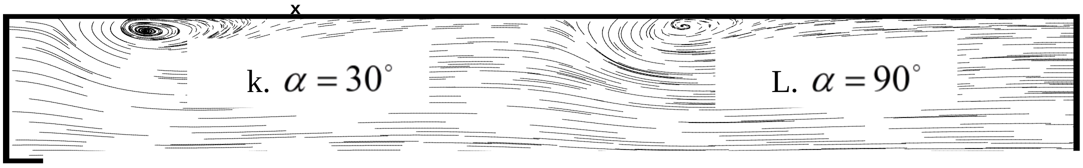

k. $\alpha = 30^{\circ}$

L. $\alpha = 90^{\circ}$

Fig.9 effect of the distance between the jets on the flow and heat transfer characteristics, Re_j =13517, Re_{in}= 16896.

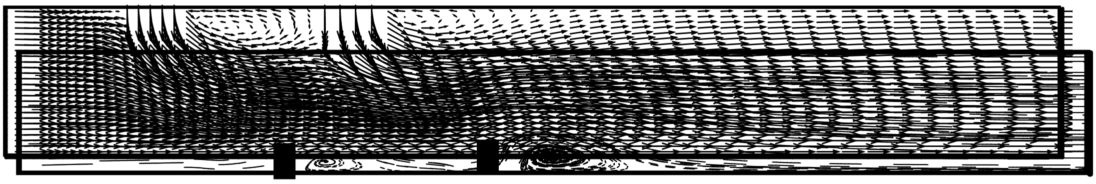

e. a. $\alpha = 30^{\circ}$, P/B=4, $\alpha = 90^{\circ}$

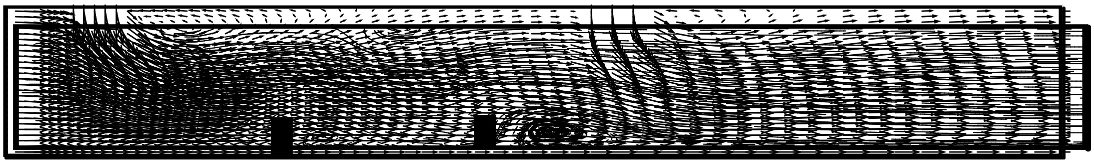

f. ve b. $\alpha = 60^{\circ}$ P/B=12, $\alpha = 90^{\circ}$

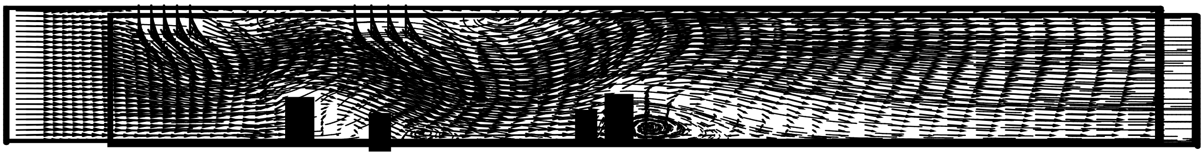

a.

c. $\alpha = 90^{\circ}$

Fig 10 streamlines for 2 jets with ribs Re_j =13517, Re_{in}= 16896, H/B=11, P/B=4, B/W=1

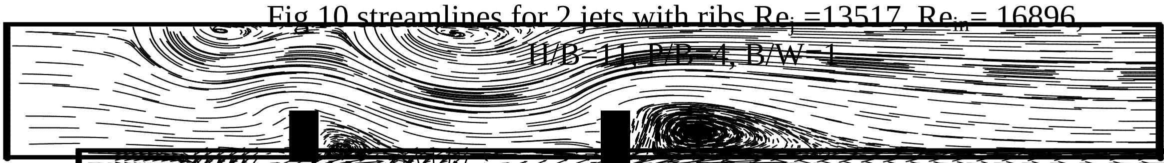

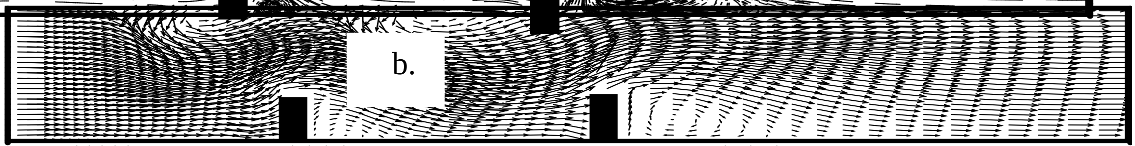

b.

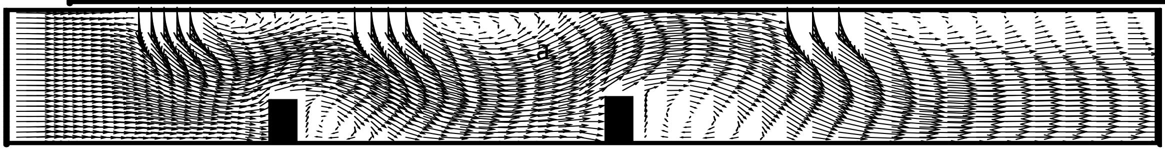

a.

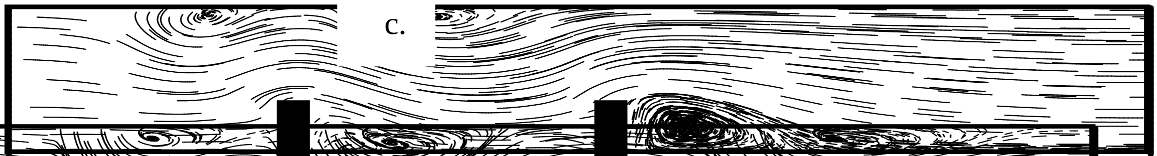

c.

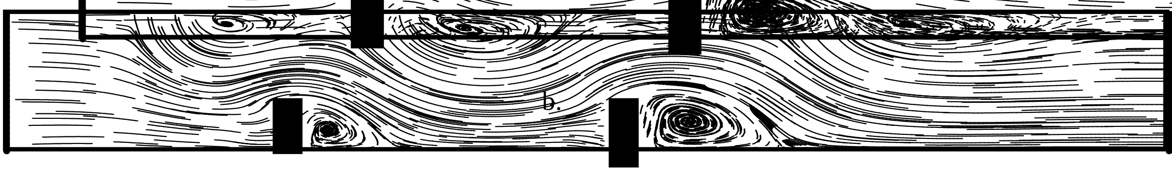

b.

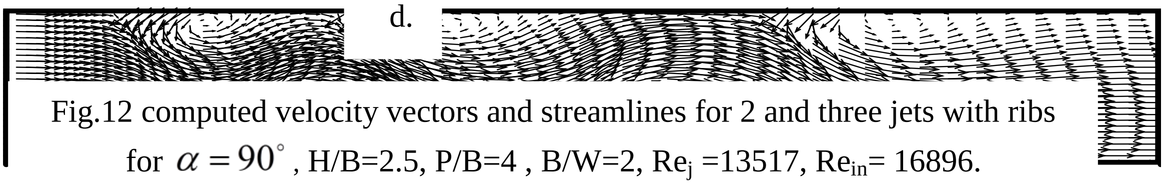

d.

Fig.12 computed velocity vectors and streamlines for 2 and three jets with ribs for $\alpha = 90^{\circ}$, H/B=2.5, P/B=4 , B/W=2, Re_j =13517, Re_{in}= 16896.

c.

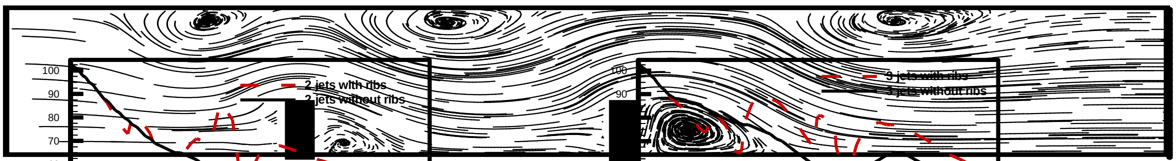

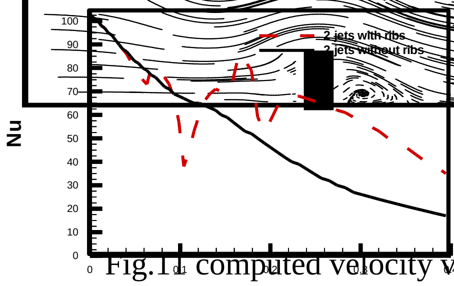

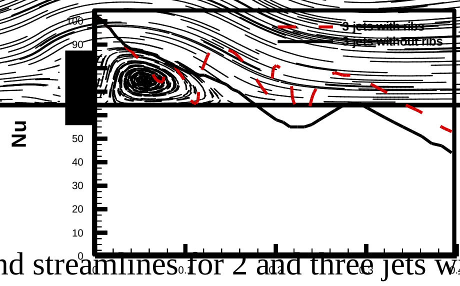

d.

Fig.11 computed velocity vectors and streamlines for 2 and three jets with ribs for $\alpha = 30^{\circ}$, H/B=2.5, P/B=4 , B/W=2, Re_j =13517, Re_{in}= 16896.

a. $\alpha = 30^{\circ}$

b. $\alpha = 30^{\circ}$

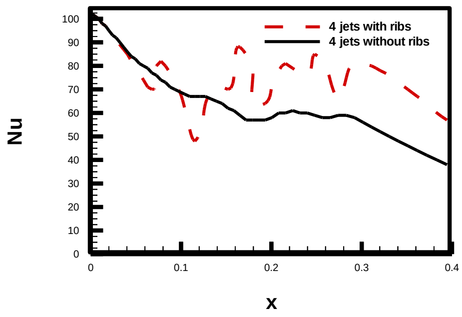

c. $\alpha = 30^{\circ}$

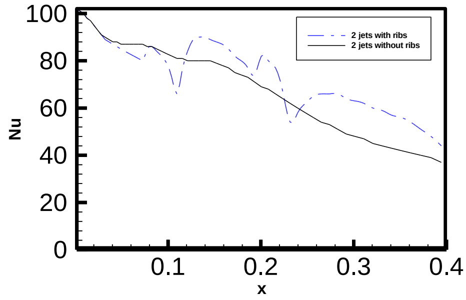

d. $\alpha = 90^{\circ}$

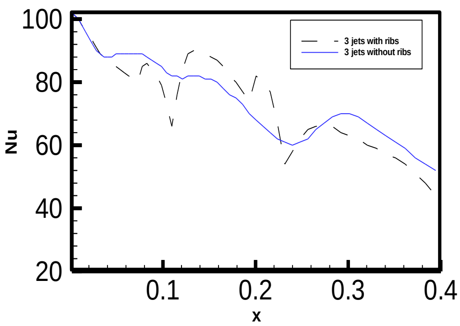

d. $\alpha = 90^{\circ}$

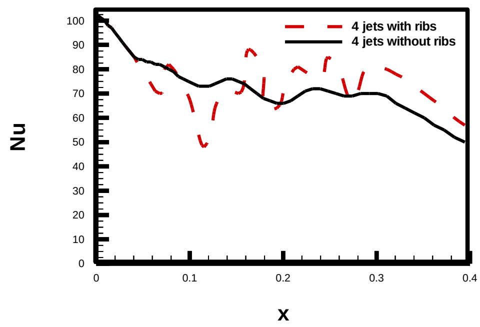

e. $\alpha = 90^{\circ}$

Fig.13. comparison of Nu number in cross flow with and without ribs (H/B=2.5, B/W=2).

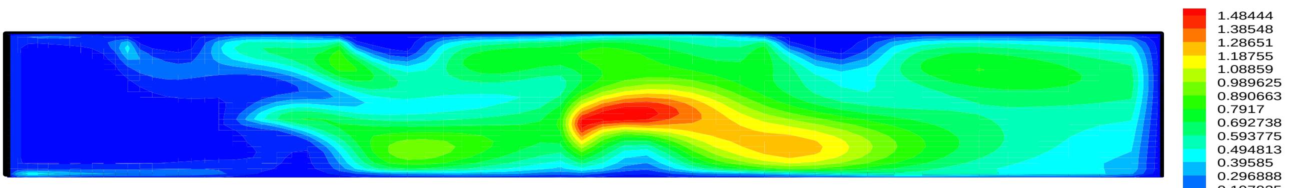

a. $\alpha = 30^{\circ}$

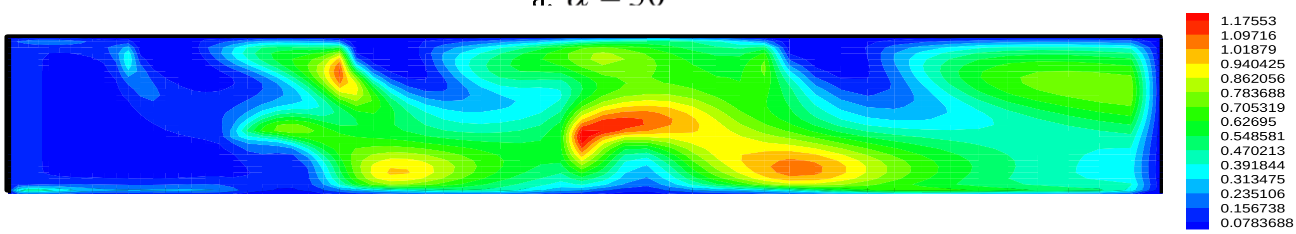

b. $\alpha = 60^{\circ}$

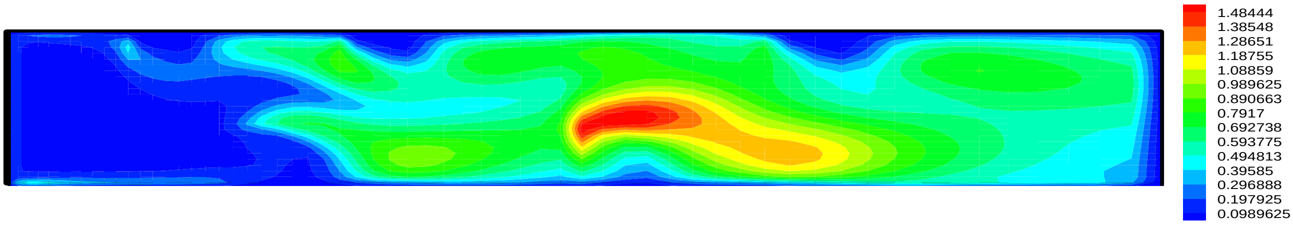

c. $\alpha = 90^{\circ}$

Fig.14 turbulent kinetic energy for 3 jets with ribs, H/B=2.5, B/W=2, Re_j =13517, Re_{in}= 16896.

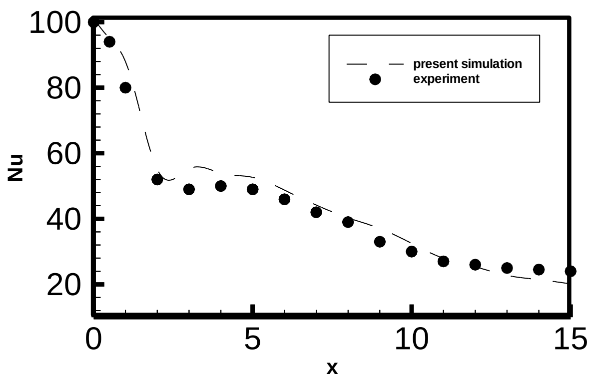

(a) impinging cooling, one jet [21], H/B=1, Re_j=6000

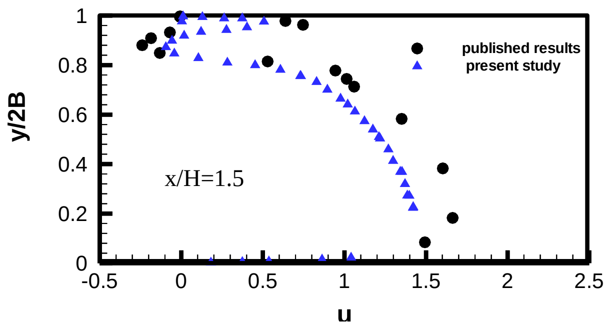

(b) published results of Lio et al.[13], turbulent cooling, H/B=1,

Fig.15. comparison between the present simulation and published experimental data.

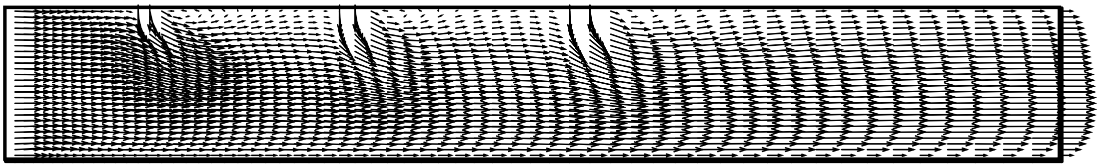

a. Rej=6210.

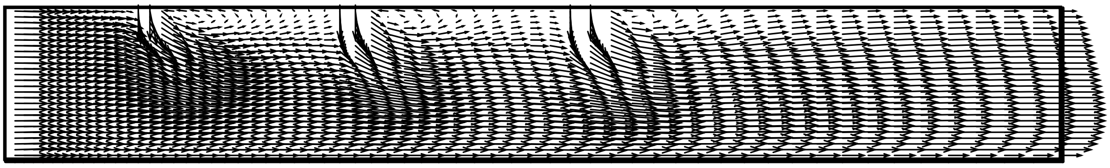

b. Rej=13517

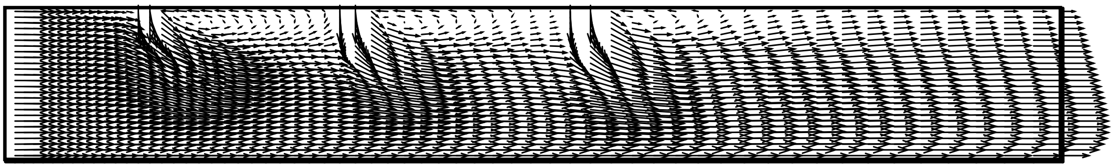

c. Rej=28127.

Fig.16 effect of Reynolds number on the computed flow field for 3 jets, H/B=11, B/W=1, $\alpha = 90^{\circ}$

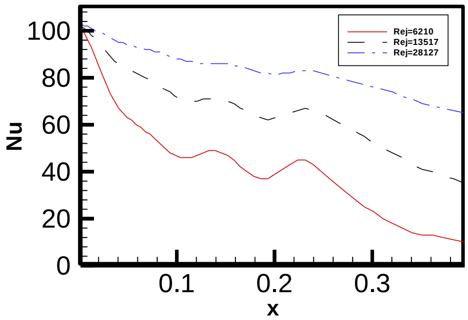

Fig.17. effect of Reynolds number on Nusselt number, for 3 jets, H/B=11, P/B=4, $\alpha = 90^{\circ}$

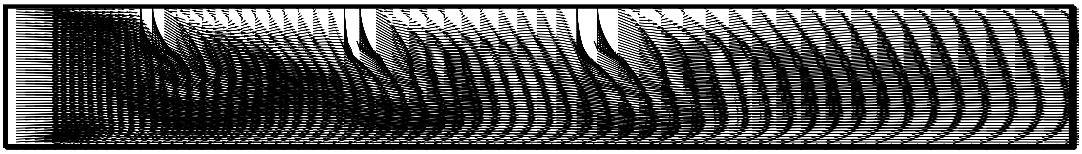

a. flow field, mesh= 62×52, $\alpha = 90^{\circ}$

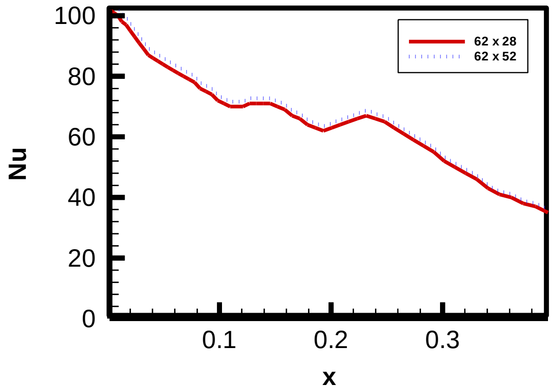

b. Nu variation for three impinging slot jets, $\alpha = 90^{\circ}$

Fig.18. effect of increasing grid nodes on the studied parameters.